



Universiteit
Leiden
The Netherlands

The interaction of water and hydrogen with nickel surfaces

Shan, J.

Citation

Shan, J. (2009, November 11). *The interaction of water and hydrogen with nickel surfaces*. Retrieved from <https://hdl.handle.net/1887/14365>

Version: Corrected Publisher's Version

License: [Licence agreement concerning inclusion of doctoral thesis in the Institutional Repository of the University of Leiden](#)

Downloaded from: <https://hdl.handle.net/1887/14365>

Note: To cite this publication please use the final published version (if applicable).

Chapter 6

Adsorption of molecular hydrogen on an ultrathin layer of Ni(111) hydride

We have used high resolution electron energy loss spectroscopy and temperature-programmed desorption to study the interaction of atomic hydrogen with Ni(111). Our results agree mostly with previous reports. We find that exposing Ni(111) to atomic hydrogen below 90 K leads to a 125 K TPD feature and two additional HREELS losses. Isotopic exchange studies lead us to attribute these features to molecular hydrogen bound to an ultrathin nickel hydride layer formed on the surface. We suggest that such binding is induced by reversible surface roughening that accompanies the phase change between the metallic nickel and the ultrathin nickel hydride layer.

6.1 Introduction

Chemisorbed molecular states for H_2 on metal surfaces are rare and mostly associated with considerable surface roughness. In recent years, theoretical studies have indicated that H_2 may bind chemically, but without dissociation, near steps at otherwise well-ordered metal surfaces, e.g. Pd(210) [1], Pt(211) [2] and even on Pd(110) [3]. Direct experimental evidence for chemisorbed molecular states has emerged from HREELS and TPD studies for H_2 adsorption on Ni(510) [4] and Pd(210) [5]. Such a molecular state may act as a precursor state and thus be of crucial importance to the dynamics of hydrogen dissociation. For example, results from experimental and theoretical studies for H_2 dissociation on Pt(211) [2,6] indicate that molecular chemisorption wells in the potential energy surface dominate dissociation at low impact energies.

The interaction of H_2 with Ni(111) has attracted attention as nickel has found widespread application in hydrogenation processes. Hydrogen dissociates on this surface with a low reaction barrier, although large exposures are necessary for (nearly) complete saturation [7-10]. The saturation coverage is generally agreed to be 1.0 monolayer (ML) [8-10], with hydrogen atoms adsorbing, especially at higher coverages, into fcc three-fold hollow sites [8,10,11-15]. Supersonic molecular beam [15] and temperature programmed desorption (TPD) studies [16] report no isotopic dependence in dissociative adsorption or associative desorption. Desorption generally occurs in two peaks near 330 K and 370 K and is very sensitive to contamination and defects [17]. A well-ordered, clean and defect-free Ni(111) surface is characterized by a ~ 40 K difference between the two desorption maxima.

Although surface-bound H does not diffuse into subsurface sites, Ceyer and co-workers showed that subsurface hydrogen atoms can be created under UHV conditions by impinging atomic hydrogen onto Ni(111) [18,19]. We refer to such a surface filled by subsurface hydrogen as an *ultrathin nickel hydride layer*. Formation of bulk nickel hydride is endothermic by 0.17 eV per H atom in the low concentration limit [20] and, consequently, an ultrathin nickel hydride layer is expected to decompose well below room temperature under vacuum conditions. In their TPD spectra, Ceyer and coworkers indeed observe two additional TPD features at 185 and 215 K. Using atomic hydrogen or ion sources, other groups have also observed TPD features well below the surface desorption

temperatures and attributed them to recombinative desorption of interstitial hydrogen [21-23].

HREEL spectra of such ultrathin nickel hydride layers show a feature centered at ~ 100 meV, in addition to features resulting from surface-bound hydrogen at 145 and 119 meV [18,24]. Subsurface hydrogen has been reported to be extremely active in hydrogenation of simple hydrocarbons [19,23,25-29] and it has found use as a titrant in experiments showing that mode-selected vibrational excitation of the C-H bond in gas-phase CHD_3 prior to impact with a thin nickel deuteride film leads primarily to C-H bond cleavage [30]. Recent debate focuses on the mechanism by which interstitial hydrogen reacts with surface-bound species to form gaseous products [12,13,19,31-34].

Hydrogen has also been reported to bind molecularly to nickel, although significant surface corrugation is required. Andersson and coworkers reported an additional H_2 TPD feature at 125 K after exposing a clean Ni(510) surface to molecular hydrogen [4]. They attributed this TPD feature to molecularly bound hydrogen based on the observation of HREELS features at 28 and 398 meV for H_2 and corresponding features at 23 and 345 for HD and 21 and 289 meV for D_2 . These features were attributed to correspond to a bending mode and the H-H stretch, respectively.

In this chapter, we report that molecular hydrogen binds to an ultrathin nickel hydride layer prepared from Ni(111). TPD experiments indicate recombinative desorption of subsurface H and surface H, and molecularly bound H_2 . HREEL spectra at 85 K show losses at energies previously reported for interstitial atomic hydrogen, surface-bound atomic H, and surface-bound molecular H_2 . When using mixed atomic hydrogen and deuterium beams to prepare the thin nickel hydride layer, we find an additional energy loss indicative of molecular HD. Combined with the observation of the disappearance and reappearance of the elastically scattered electron beam from our HREEL spectrometer, we interpret our results to indicate that formation of the thin nickel hydride film at 85 K leads to enough corrugation for this surface to bind molecular hydrogen.

6.2 Experiment

Experiments are carried out in an UHV system, which consists of two chambers. The top chamber is used for preparation of the Ni(111) surface, and for TPD experiments with a

quadrupole mass spectrometer (Balzers QMS 422). The lower chamber contains an upgraded ELS 22 high resolution electron energy loss spectrometer and a double-pass CMA for Auger electron spectroscopy (Staib Instruments). The top and lower chambers are separated by a gate valve. The typical base pressure of the system is less than 1×10^{-10} mbar.

The Ni(111) single crystal, cut and polished to less than 0.1° of the low Miller-index plane (Surface Preparation Laboratories, Zaandam, the Netherlands), can be heated to 1200 K by electron bombardment and cooled to 85 K. The crystal temperature is measured by a chromel-alumel thermocouple spot-welded to the edge of the crystal. The crystal is cleaned by Ar^+ sputtering, annealing at 1100 K, followed by oxidation in 10^{-7} mbar of O_2 and reduction in 10^{-6} mbar of H_2 . After cleaning, the surface cleanliness is verified by AES. The hydrogen coverage is estimated from the TPD integral taken for $m/e=2$. We convert the integral to an absolute coverage using the intergral determined after dosing $30,000 \times 10^{-6}$ mbar*s H_2 at 85 K as a reference for 1 ML [8-10]. All TPD measurements are performed with a heating rate of 1.0 K/s. The HREEL spectra are recorded at 5 to 9 meV resolution (FWHM) with typical 1×10^4 cps for the scattered elastic peak.

We use a thermal hydrogen cracker (H-Flux, Tectra) for dosing atomic hydrogen. In this source, a heated tungsten capillary is kept at 1800 K while hydrogen flows through its orifice toward the Ni(111) surface. This cracking temperature avoids formation of tungsten vapor and provides a small radiative load onto the crystal. The distance between source and crystal in combination with a heat shield ensures that the crystal temperature remains below 90 K during dosing. At the cracking temperature of 1800 K, the dissociation fraction is estimated to be $\sim 90\%$ when the capillary pressure is below 1×10^{-5} mbar. While the atomic hydrogen beam is therefore actually a mixture of atomic and molecular hydrogen, we refer to the mixture as the atomic hydrogen beam. As a feed for the hydrogen cracker we use 5N5 H_2 (Messer) and 99.8% isotopic purity D_2 (Linde).

6.3 Results

Figure 6.1 shows a series of H_2 TPD spectra measured after exposing Ni(111) to various amounts of atomic hydrogen at 85 K. For comparison, we also show the desorption

spectrum of surface hydrogen in curve a, in which only H₂ is dosed to the maximum surface coverage. Curve a clearly shows two desorption features at 325 and 365 K, which is typical for an associative desorption spectrum of 1 ML chemisorbed hydrogen [8,9,18]. The 40 K difference in peaks testifies to the cleanliness of the surface and the absence of significant corrugation or defects [17]. In curves b, c, and d, we observe additional desorption features. Two closely-spaced peaks appear at 180 and 190 K and a small desorption feature appears at 125 K. The peaks at 180 and 190 K appear prior to the 125 K feature (compare traces b and c). The latter feature does not increase significantly with increasing atomic hydrogen dose, while the features at 180 and 190 K do (compare traces c and d). The appearance of lower temperature peaks does not significantly affect the peak positions for surface recombination at 325 and 365 K.

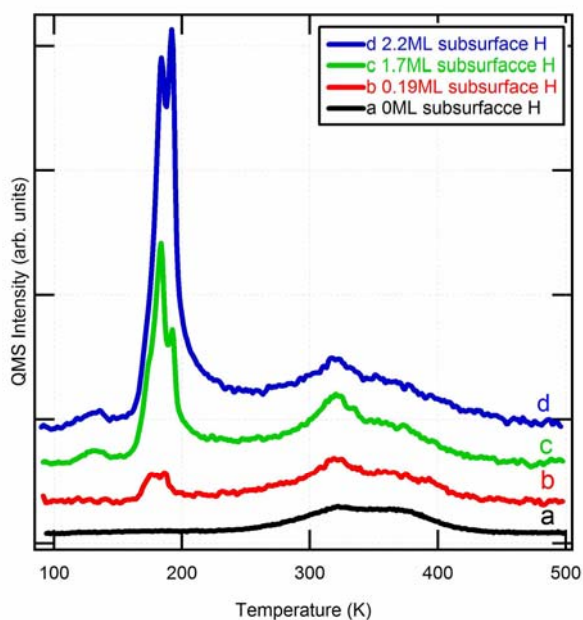


Figure 6.1 TPD spectra of $m/e=2$ measured after exposure of the Ni(111) crystal to various amounts of atomic hydrogen at 85 K.

Figure 6.2 shows two HREEL spectra measured after exposing Ni(111) at 85-90 K to atomic hydrogen (bottom trace) or atomic deuterium (top trace). The dotted line represents the

original HREELS spectra, while the solid line is a fit to this data using a summation of an exponential decay and three off-set Gaussian functions. The indicated amount of subsurface hydrogen (deuterium) is determined after the HREELS measurements from an integrated TPD spectrum. Both spectra are taken at 10° off-specular angle using an impact energy of the primary electron beam of 9.6 eV, since at this energy both surface and subsurface vibrations can be observed [18]. In the bottom trace, we distinguish four energy losses: a strong and sharp feature at 30 meV, a broader feature centered at 100 meV with peak appearing in the shoulder at 141 meV, and a broad feature centered at 420 meV. In the top trace, four energy losses appear at 24, 80, 100 and 305 meV. They show the same intensity and width variations as the features observed in the bottom trace. When repeating the experiment with atomic hydrogen, but flashing the crystal to 140 K prior to taking a HREEL spectrum, we observe the same spectrum as the bottom trace in figure 6.2 but without the 30 meV and 420 meV features.

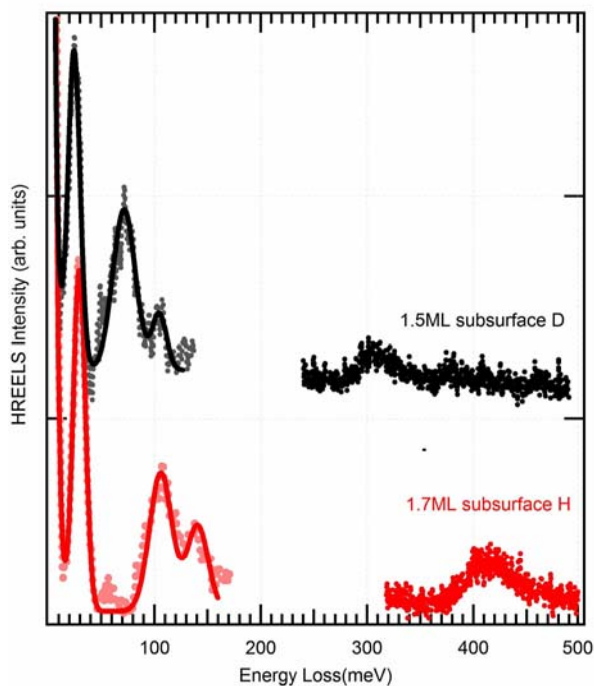


Figure 6.2 HREEL spectra collected at 85 K and at 10° off-specular angle with an impact energy of 9.6 eV. See text for details.

We have noted that preparation of the nickel hydride film at 85 K without any further treatment prior to collecting the HREEL spectrum leads to an almost complete loss of signal intensity for the elastically scattered beam. Signal intensity returns after flashing the crystal temperature to above 220 K. This suggests that formation of the nickel hydride layer at 85 K induces surface corrugation. Since the scattered intensity of the primary beam is diffuse, long signal averaging was required to collect each part of the spectra shown in figure 6.2. To minimize interfering contamination of the surface, we have therefore collected spectral information in the smaller energy regimes shown here with increased resolution. A single experiment using the H isotope and a lower resolution scanned the entire energy regime and showed no observable features in the energy window left out of the bottom trace.

Isotopic mixing of H₂ and D₂ in the feed of our thermal cracker allows us to dose H and D atoms simultaneously in combination with residual H₂, D₂ and HD. Figure 6.3 presents a HREEL spectrum taken at 85 K after dosing the clean Ni(111) surface with such a mixture. We focus here on energy regimes relevant to the interpretation of our data. Most prominently, we observe three energy losses in the higher energy regime at 305, 344 and 420 meV. Between 100 and 200 meV we observe no losses. The peak edge near 220 meV results from accumulating CO [35].

It may be suggested that the time required for signal averaging to obtain the spectra in figure 6.2 and 6.3 leads to contamination of the surface, especially by H₂O. Recently, we have studied water adsorption on (partially) hydrogen-covered Ni(111) in detail [36,37], also see Chapter 3 and 4. H₂O shows losses near 420, 200, 50-100 and 30 meV for stretching and bending vibrations, librations and frustrated translations, respectively. The relative intensities of these vibrations are such that when the O-H stretch is observed, the librations between 50-100 meV are more prominent in both specular and off-specular HREEL spectra [36]. Since in figure 6.2 the librations of water are not present, we conclude that the observed features are not due to H₂O. Also, flashing the crystal to 140 K prior to taking HREEL spectra should not lead to a loss of vibrational features of water, as any amount of water on (hydrogen-covered) Ni(111) does not desorb until >150 K [36]. Finally,

the presence of the 344 meV in figure 6.3 cannot be accounted for by a (deuterated) water isotope, and water contamination would have appeared by bending modes of (deuterated) water in the 100-220 meV window.

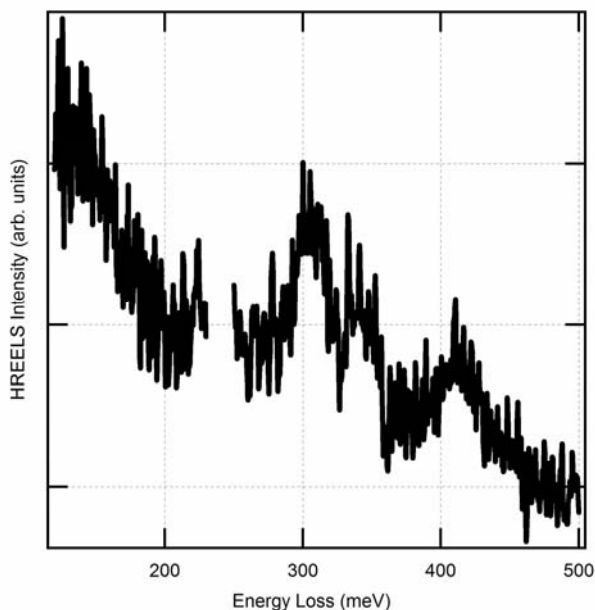


Figure 6.3 HREEL spectra region for H₂, D₂, and HD stretch region, as well as water bending mode region.

6.4 Discussion

First, we focus our attention on the TPD spectra in figure 6.1. As mentioned, in curve a only H₂ is dosed. The double peak feature at 325 K and 365 K is typical for desorption of 1 ML surface hydrogen. In curves b, c, and d atomic dosing is used and the same peaks appear, while additional maxima appear at 180 K and 190 K. The integral of the feature at 180-190 K reaches 1.7 and 2.2 surface monolayers in c and d, respectively. In previous publications, desorption of subsurface hydrogen from ultrathin nickel hydride layers was reported in similar temperature regimes [18,19,21-22]. Following this earlier assignment, we attribute these TPD maxima to ‘resurfacing’ hydrogen from interstitial sites with immediate reaction with surface-bound hydrogen to form H_{2(g)}. We note that the appearance

of H₂ in the gas phase at this temperature may also be interpreted as resulting from a phase transition of the ultrathin nickel hydride film to metallic nickel with a surface layer of atomically bound hydrogen. Since desorption of surface-bound hydrogen is sensitive to defects [17] the lack of changes in the 325 and 365 K features indicates that this reversible phase change does not lead to many defects at the Ni(111) surface.

When comparing our TPD spectra with the earliest report, we find that the width of the subsurface hydrogen features in our spectra is considerably narrower [18]. Although we cannot offer conclusive evidence at this point, we expect that it results from different procedures used to prepare the ultrathin nickel hydride film. Whereas the surface temperature remains below 90 K during exposure to atomic hydrogen in our experiments, other studies indicate that the crystal temperature increased to 130 K during dosing. This also explains why the 125 K TPD feature appearing in traces c and d was not observed in previous studies of this system.

Regarding the 125 K feature in our TPD traces, which amounts to ~0.15 ML in traces c and d and which does not increase noticeably in size when increasing the atomic hydrogen exposure, we note that such a low temperature peak for H₂ desorption has not been identified before for H₂/Ni(111). To our knowledge, only Andersson and coworkers observed a similar peak for hydrogen at 125 K when Ni(510) was exposed to molecular hydrogen [4]. On the basis of HREEL spectra, this TPD peak was attributed to desorption of molecular hydrogen bound to steps on the Ni(510) surface.

As mentioned in the introduction, two HREELS features at 145 meV and 119 meV are observed for the hydrogen-saturated Ni(111) surface. We also observe these features when we only dose H₂. Subsurface hydrogen yields an additional broad feature centered at 100 meV in HREEL spectra [18]. In figure 6.2, we ascribe the 100 and 141 meV features to subsurface and surface H, respectively. This assignment is in line with the expected isotope shift observed in the top trace in figure 6.2 when using D atoms. The broad feature centered at 80 meV is ascribed to subsurface D, while the small feature at 100 meV is ascribed to surface D.

In figure 6.2, we are left with two features at 30 (24) and 420 (305) meV for hydrogen (deuterium). The energy, shape and relative intensity of these losses compare well to those

observed for molecular hydrogen adsorbed on Ni(510) [30]. In that study, a broad feature centered at 398 meV (289 meV) was attributed to the stretch vibration of H₂ (D₂), while a sharp and intense peak at 28 (21) meV was assigned to the bending mode of Ni-H₂ (Ni-D₂) [4]. On Pd(210), molecular hydrogen adsorption has also been detected by TPD and HREELS [5]. Here, a feature near 420 (300) meV was suggested to result from the H-H (D-D) stretch vibration. Finally, ionic Ni₄⁺ clusters created in a deuterium atmosphere bind molecular D₂ resulting in an IR active D-D stretch vibration at 305 meV [38]. The resemblance of all these observations to ours suggests that the 420 (305) meV feature in our spectra results from an internal H₂ (D₂) stretch of molecular hydrogen bound to the ultrathin nickel hydride (deuteride) film, while the 30 (24) meV feature results from a Ni-H₂ (Ni-D₂) bend. The disappearance of these peaks when flashing the crystal to 140 K prior to taking a HREEL spectrum connects the 125 K TPD feature to these particular energy losses and provides further evidence that H₂ is present at the surface after preparing the ultrathin nickel hydride layer at 85-90 K.

Finally, we turn to the HREEL spectrum in figure 6.3 which was taken after dosing a combination of H and D atoms. Of the three losses observed, the 305 and 420 meV features also occur when dosing only D or H (Figure 6.2) and likely result from the same vibrational modes and the same species. For the feature at 344 meV, a similar feature was observed when dosing HD on Ni(510) at 345 meV and the relative energies suggest that this experiment created H₂, HD and D₂ simultaneously at the ultrathin nickel hydride (deuteride) surface. Thus, we conclude that experiments in which the atomic hydrogen beam impinges on Ni(111) near 85 K produces molecularly bound hydrogen. This molecularly bound hydrogen desorbs at 125 K.

Finally, we are left to consider what changes the Ni(111) surface when forming an ultrathin nickel hydride layer such that it binds molecular hydrogen. The early studies on Ni(510) concluded that molecular hydrogen adsorbs at the steps of the nickel surface. We detect molecular hydrogen only when subsurface hydrogen is present in otherwise flat Ni(111). We also noted that exposing the crystal to atomic hydrogen at 85 K leads to an almost complete disappearance of signal intensity for the elastically scattered electron beam, which only reappears above 220 K, when all subsurface hydrogen has desorbed. The

combination of these observations suggests that formation of the ultrathin nickel hydride layer near 85 K induces corrugation and roughening that allows for molecular H₂ adsorption. As formation of nickel hydride from pure nickel expands the nickel lattice with 2.9 Å³ per hydrogen atom up to x=0.7 in NiH_x [20], upward relaxation of surface nickel atoms is expected upon formation of a ultrathin nickel hydride layer on Ni(111). Such relaxation has been observed by STM for small quantities of subsurface hydrogen absorbed in Pd(111) [39]. Pd shows the same volume change per H atom in this regime of hydride formation [20]. A similar relaxation on Ni(111) would explain the loss of the elastically scattered electron beam intensity and provides adsorption sites for H₂ that resemble steps on Ni(510) and edge atoms in cationic Ni₄ clusters. Also, the recovery of the scattered elastic peak intensity above 220 K is in line with decomposition of a slightly corrugated ultrathin nickel hydride film, leading back to a smooth Ni(111) surface. Significant transport of Ni atoms (e.g. as NiH or NiH₂) along the surface in this reversible process of ultrathin hydride formation may be excluded as the reverse phase change to Ni(111) would have left the surface roughened with an accompanying change in the H₂ surface desorption features at 325 and 365 K in traces 1c and d. Also, the scattered elastic electron beam intensity would not have recovered.

6.5 Conclusions

We have demonstrated that dosing atomic hydrogen on Ni(111) at a surface temperature below 90 K leads to molecular hydrogen bound to an ultrathin nickel hydride layer. We suggest that the adsorption of molecular hydrogen is due to reversible roughening associated with formation of the NiH_x layer. However, the roughening is modest and likely consists only of relaxation of nickel atoms normal to the surface. The newly found molecular state of hydrogen persists to 125 K and may present an interesting case to study H₂ reaction and scattering dynamics.

6.6 References

- [1] M. Lischka, and A. Groß, *Phys. Rev. B*, 2002, **65**, 075420.
- [2] D. A. McCormack, R. A. Olsen, and E. J. Baerends, *J. Chem. Phys.*, 2005, **122**, 194708.
- [3] H. F. Busnengo, W. Dong, and A. Salin, *Phys. Rev. Lett.*, 2004, **93**, 236103.
- [4] A.-S. Mårtensson, C. Nyberg, and S. Andersson. *Phys. Rev. Lett.*, 1986, **57**, 2045.
- [5] P. K. Schmidt, K. Christmann, G. Kresse, J. Hafner, M. Lischka, and A. Groß, *Phys. Rev. Lett.*, 2001, **87**, 096103.
- [6] I. M. N Groot, K. J. P. Schouten, A. W. Kleyn, and L. B. F. Juurlink, *J. Chem. Phys.*, 2008, **129**, 224707.
- [7] K. Christmann, O. Schober, G. Ertl, and M. Neumann, *J. Chem. Phys.*, 1974, **60**, 4528.
- [8] K. Christmann, R. J. Behm, G. Ertl, M. A. Van Hove, and W. H. Weinberg, *J. Chem. Phys.*, 1979, **70**, 4168.
- [9] A. Winkler, and K. D. Rendulic, *Surf. Sci.*, 1982, **118**, 19.
- [10] K. Mortensen, F. Besenbacher, I. Stensgaard, and W. R. Wampler, *Surf. Sci.*, 1988, **205**, 433.
- [11] B. Bhatia, and D. S. Sholl, *J. Chem. Phys.*, 2005, **122**, 204707.
- [12] J. Greeley, and M. Mavrikakis, *Surf. Sci.*, 2003, **540**, 215.
- [13] R. Baer, Y. Zeiri, and R. Kosloff, *Phys. Rev. B*, 1997, **55**, 10952.
- [14] H. Yanagita, J. Sakai, T. Aruga, N. Takagi, and M. Nishijima, *Phys. Rev. B*, 1997, **56**, 14952.
- [15] A. C. Luntz, J. K. Brown, and M. D. Williams, *J. Chem. Phys.*, 1990, **93**, 5420.
- [16] K. Christmann, *Surf. Sci. Rep.*, 1988, **9**, 1.
- [17] K. D. Rendulic, A. Winkler, and H. P. Steinrück. *Surf. Sci.*, 1987, **185**, 469.
- [18] A. D. Johnson, K. J. Maynard, S. P. Daley, Q. Y. Yang, and S. T. Ceyer, *Phys. Rev. Lett.*, 1991, **67**, 927.
- [19] S. T. Ceyer, *Acc. Chem. Res.*, 2001, **34**, 737.
- [20] Y. Fukai, The metal-hydrogen system, 1993, Springer-Verlag, Berlin.
- [21] H. Premm, H. Pölzl, and A. Winkler, *Surf. Sci. Lett.*, 1998, **401**, L444.
- [22] S. Wright, J. F. Skelly, and A. Hodgson, *Faraday Discuss.*, 2000, **117**, 133.
- [23] A. T. Capitano, and J. L. Gland, *Langmuir*, 1998, **14**, 1345.
- [24] H. Okuyama, T. Ueda, T. Aruga, and A. M. Nishijima, *Phys. Rev. B*, 2001, **63**, 233404.
- [25] A. D. Johnson, S. P. Daley, A. L. Utz, and S. T. Ceyer, *Science*, 1992, **257**, 223.
- [26] S. P. Daley, A. L. Utz, T. R. Trautman, and S. T. Ceyer, *J. Am. Chem. Soc.*, 1994, **116**, 6001.
- [27] K. L. Haug, T. Bürgi, T. R. Trautman, and S. T. Ceyer, *J. Am. Chem. Soc.*, 1998, **120**, 8885.

Adsorption of molecular hydrogen on an ultrathin layer of Ni(111) hydride

- [28] K. L. Haug, T. Bürgi, M. Gostein, T. R. Trautman, and S. T. Ceyer, *J. Phys. Chem. B.*, 2001, **105**, 11480.
- [29] A. T. Capitano, K.-Ah. Son, and J. L. Gland, *J. Phys. Chem. B.*, 1999, **103**, 2223.
- [30] D. R. Killelea, V. L. Campbell, N. S. Shumann, and A. L. Utz, *Science*, 2008, **319**, 790
- [31] V. Ledentu, W. Dong, and P. Sautet, *J. Am. Chem. Soc.*, 2000, **122**, 1796.
- [32] A. Michaelides, P. Hu, and A. Alavi, *J. Chem. Phys.*, 1999, **111**, 1343.
- [33] G. Henkelman, A. Arnaldsson, and H. Jónsson. *J. Chem. Phys.*, 2006, **124**, 044706.
- [34] S. Wright, J. F. Skelly, and A. Hodgson, *Chem. Phys. Lett.*, 2002, **364**, 522.
- [35] W. Erley, H. Wagner, and H. Ibach, *Surf. Sci.*, 1979, **80**, 612.
- [36] J. Shan, J. F. M. Aarts, A.W. Kleyn, and L. B. F. Juurlink, *Phys. Chem. Chem. Phys.*, 2008, **10**, 2227; this thesis chapter 3.
- [37] J. Shan, J. F. M. Aarts, A.W. Kleyn, and L. B. F. Juurlink, *Phys. Chem. Chem. Phys.*, 2008, **10**, 4994; this thesis chapter 4.
- [38] I. Swart, P. Gruene, A. Fielicke, G. Meijer, B. M. Weckhuysen, and F. M. de Groot, *Phys. Chem. Chem. Phys.*, 2008, **10**, 5743.
- [39] E. C. H. Sykes, L. C. F-Torres, S. U. Nanayakkara, B. A. Mantooth, R. M. Nevin, and P. S. Weiss, *PNAS*, 2005, **102**, 17907.

